Paper 201

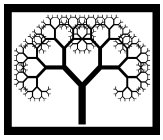

Proceedings of the Eleventh International Conference
on Computational Structures Technology,
B.H.V. Topping, (Editor),
Civil-Comp Press, Stirlingshire, Scotland

Evaluation of Seismic Energy Demand of Reinforced Concrete Moment Reistant Frames Considering Soil-Structure Interaction Effects

S. Gharehbaghi[1], E. Salajegheh[2] and M. Khatibinia[2]
[1] Department of Civil Engineering
Islamic Azad University, Shoushtar Branch, Iran
[2] Department of Civil Engineering
Shahid Bahonar University of Kerman, Iran

Abstract

This paper deals with the evaluation of seismic behaviour of reinforced concrete moment resistant frames (RC-MRFs) considering soil-structure interaction (SSI) effects. In this study, a three-bay nine-storey RC-MRF is optimally designed based on the design codes recommendations. To investigate the SSI effects on the seismic behaviour of the frame, a direct method is used for the modelling of SSI system. Six ground motion records are used; and the seismic behaviour of the SSI system is compared with those of RC-MRF without the SSI effects. To achieve this purpose, hysteretic energy demand and inelastic inter-story drift ratio over the height of structure are considered as the comparison criterion.

Keywords: seismic evaluation, soil-structure interaction, hysteretic energy, inelastic inter-story drift ratio, optimisation.

1 Introduction

Over the past decades, seismic performance evaluation of structures has been widely performed in line with the retrofitting, rehabilitation of structures and development of seismic design codes. The parameters that are usually used for seismic performance evaluation of structures are the inelastic inter-storey drift ratio and plastic hinge rotation at the each end section of structural elements. In addition to the mentioned parameters, the parameters based on energy concepts including input and hysteretic energy demand of structures during an earthquake excitation can be used for this purpose.

One of the most important problems in the seismic evaluation of structures is the effects of soil dynamic behaviour. During an earthquake, soil-structure interaction (SSI) effects play an important role in the seismic behaviour of structures constructed on the relatively soft soil. Accordingly, the soft soil under structures alters the actual nonlinear dynamic behaviour of the structures. Hence, SSI effects

between soil and structure should be considered in the seismic behaviour of structures [1, 2].

Many researchers considered estimating the SSI effects on elastic response of structures. However, a few considerable attentions have been regarded on the inelastic response of structures. The effect of SSI on damage in a Bilinear-SDOF model was investigated under seismic loading [3]. It is shown that the SSI substantially increases the damage index of short-period buildings located on soft soils. Inelastic displacement ratios and ductility demands were investigated for SDOF systems with period range of 0.1-3.0(s) with nonlinear behaviour considering SSI effect [4]. Lu *et al.* [5] considered the conditions of consideration of SSI for ordinary RC frames with circular mat foundations supported at the surface, embedded foundations of circular shape, and embedded foundations of arbitrary shapes. Performance based assessment of building frames with SSI effects also was considered by Fatahi *et al.* [6]. In this study, a fifteen storey moment resisting building frame was selected in conjunction with three different soil deposits with shear wave velocity less than 600(m/s). It was shown that performance levels of the structures change from life safety to near collapse when dynamic SSI is incorporated. Also, the effects of SSI were considered on the seismic response of coupled wall-frame structures on pile foundations designed according to modern seismic provisions [7]. Comparisons of the results obtained considering compliant base and fixed base models also were presented by addressing the effects of SSI on displacements, base shears, and ductility demand. The influence of inelastic dynamic SSI was investigated on the seismic vulnerability assessment of buildings [8]. The seismic vulnerability was evaluated in terms of analytical fragility curves constructed on the basis of non-linear dynamic finite elements analysis.

This paper deals with the evaluation of seismic behaviour of RC Moment Resistant Frames (MRFs) considering SSI effects. To achieve the purpose, hysteretic energy demand and inelastic inter-story drift ratio over the height of structures are considered to control the seismic demand of structure. To evaluation the seismic behaviour of RC-MRFs considering SSI effects, three-bay nine-storey RC-MRF optimally designed based on design codes recommendations is considered. The construction cost is regarded as an objective function and the frame is designed using optimisation technique. Discrete particle swarm optimisation (DPSO) algorithm proposed by Salajegheh *et al*. [9] is utilized to perform the optimisation process. Six strong ground motion records are selected for the evaluation of seismic energy demand of the frame. Consequently, the inelastic inter-storey drift ratio and hysteretic energy demand of the frame for each record are compared with and without considering SSI effects. The numerical results show that SSI effects are of great importance in the seismic evaluation of RC-MRF constructed on the relatively soft soil.

2 Seismic energy evaluation

During some natural events such destructive earthquakes as the 1971 San Fernando, 1994 Northridge, 1995 Kobe earthquakes and so forth, many structures suffered major damage. Researchers and engineers in structural and earthquake engineering

field developed innovative and practical design methodologies to assure suitable seismic performance for the structures during earthquake. Among these design methodologies, one can be referred to performance-based seismic design (PBSD) and also energy-based seismic design approaches. The conceptual framework for PBSD has been developed over the last 15 years by various guidelines such as SEAOC Vision-2000, ATC-40 and FEMA-356 [10-12]. The main objective of PBSD specified the desired seismic performance target for the structure against natural hazards. A performance objective comprises two parts: a level of performance typically can be uttered in terms of a damage state and a hazard level describing the expected seismic loads at the site. The performance levels include collapse prevention, life safety, and immediate occupancy of the building following the design seismic event [13, 14].

There are more rational seismic design alternatives such as energy-based seismic design which was proposed by Housner [15]. The method is based on a balance between the energy demand during earthquake and energy supply of structure as the structural system. Actually, the method implies that the energy supply should be more than the energy demand. The energy-based seismic design approach has been extensively attended and developed it since 25 years. Akiyama [16], Kuwamura and Galambos [17] measured the amount of input energy of structures due to several earthquake ground motions. Concluded from their studies, the hysteretic energy demand is a good parameter for the clarification of structural demands and damages. Uang and Bertero [18], Bertero and Uang [19] also stipulated the exploit of the seismic energy as a reliable parameter in seismic design of structures. As well, they emphasized that researchers develop the energy concepts to use in seismic design codes. Chung and Uang [20] offered two types of formulation for computing input energy. It was shown that there is significant distinction between the profiles of the energy time histories calculated by the absolute energy and by those of the conventional relative energy equation.

Khashaee [21] investigated the influences of the soil and ground motion characteristics such as severity, duration and frequency content on earthquake input and hysteretic energies as well as their distributions in steel structures. In this study, it is recognized that the soil and ground motion characteristics have a major influence on the amount of energy transmitted to a building, but a minor influence on how the energy is distributed through the height. In addition, the structural systems such as fixed base, supplemental damping and base-isolation influence the amount and distribution of energy in structures**.** Moreover, it was emphasised that the use of energy concepts should be considered in seismic design codes [22]. Recently, Gong *et al.* [23], Gharehbaghi and Salajegheh [24], Gharehbaghi [25] and Gharehbaghi *et al.* [26] used the seismic energy concepts including input energy and hysteretic energy dissipation in design optimisation of structures.

2.1 Energy-based seismic evaluation

At the first time, Housner proposed the idea of energy-based seismic design [15]. When ground motion transmits energy into a structure, some of the energy is dissipated through damping and non-linear behaviour. The remainder energy of the

structure is stored in the form of kinetic energy and elastic strain energy. Accordingly, it can be written:

$$E_K(t) + E_D(t) + E_A(t) = E_I(t) \tag{1}$$

where $E_I(t)$, $E_K(t)$ and $E_D(t)$ are explanatory the energy demand, kinetic energy and damping energy, respectively; $E_A(t)$ encompasses the recoverable elastic strain energy ($E_S(t)$) and the irrecoverable plastic hysteretic energy ($E_H(t)$). Amount of $E_H(t)$ is equal to zero in elastic systems and is appeared in inelastic systems. Therefore, Equation (1) can be expressed as:

$$E_K(t) + E_D(t) + E_S(t) + E_H(t) = E_I(t) \tag{2}$$

where $E_A(t)$ and $E_S(t)$ are cumulative during ground motion and are vanished at the end of motion for inelastic systems. These terms are very small in comparison with $E_D(t)$ and $E_H(t)$. Thus, the most portion of energy demand is dissipated as damping and hysteretic energies while Equation (2) can be approximately written as:

$$E_D(t) + E_H(t) \cong E_I(t) \tag{3}$$

According to the equation, the main portion of input energy demand is converted to the damping and hysteretic energy. Besides, if the structural system remains in elastic range during earthquake, $E_H(t)$ is trivial and the energy-based analysis is not useful for design [27].

2.2 Hysteretic energy dissipation (HED)

Actually, the most important portion of energy equation is HED. Inelastic cyclic deformations are occurred in structural elements when subjected to the strong ground motions. This is caused the structural elements dissipate the portion of input energy trough inelastic cyclic deformations. It is generally recognized that the level of structural damage is due to cumulative damage that creates by inelastic cyclic deformations. Therefore, HED is the structural response parameter supposed that can correlated to cumulative damage closely. Amount of dissipated energy related to each element should not be more than the fraction of its HED capacity. If the equilibrium is not satisfied, structural elements sustain significant damage. In addition, HED should not be concentrated in special elements or stories. Hence, the identification and controlling of HED demand has much effect on structural seismic behaviour.

In the energy-based seismic design approach based on energy concepts and the equilibrium of absorbed and dissipated energies, effects of the parameters such as ground motion duration, inelastic excursions, strength and stiffness deterioration etc, can be considered. The consideration of the effects is caused the structural seismic

behaviour is close to reality. Housner [15] expressed that the energy supply should be more than the energy demand during earthquake for controlling and avoidance of the structural collapse. Thus, the investigation of seismic energy demand of structures is of great importance during earthquake.

3 SSI system definition

3.1 Seismic responses of SSI system

Direct method and substructure method have been suggested for modelling of SSI system [28]. In this study, the direct method is considered. In this method, discretized dynamic equations of structure and soil are considered simultaneously. Therefore, responses of soil and structure are determined simultaneously by analyzing SSI system in each time step [28]. The infinite boundaries of soil are modelled using the artificial boundaries (Figure 1).

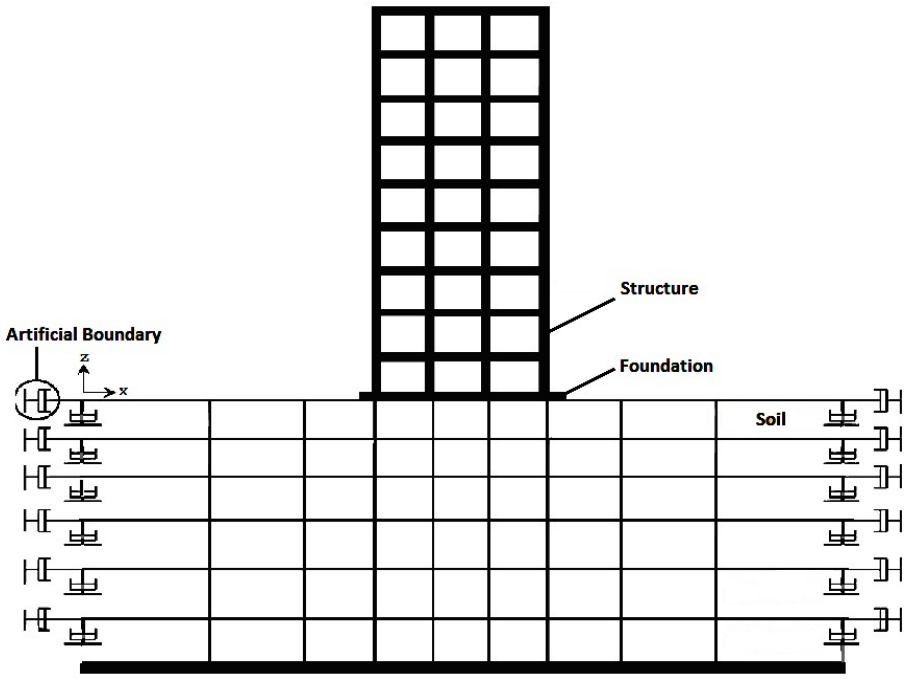

Figure 1: Modelling configuration of SSI system using direct method.

The nonlinear discretized dynamic equations of 2-D SSI system subjected to seismic excitation can be formulated in FEM framework as:

$$\boldsymbol{M}\,\Delta\ddot{\boldsymbol{u}} + \boldsymbol{C}\,\Delta\dot{\boldsymbol{u}} + \boldsymbol{K}_T\,\Delta\boldsymbol{u} = -\boldsymbol{m}_x\,\ddot{\boldsymbol{u}}_{g,x}(t+\Delta t) - \boldsymbol{F}(t) \tag{4}$$

where $\boldsymbol{M}, \boldsymbol{C}$ and $\boldsymbol{K}_T$ are mass, damping and tangent stiffness matrices of SSI model, respectively; $\Delta\boldsymbol{u}$ is the incremental vector of the relative displacements for SSI

system between times t and $t+\Delta t$; and $\boldsymbol{F}(t)$ is the vector of internal forces at time t. The term $\ddot{\boldsymbol{u}}_{g,x}(t+\Delta t)$ is the free-field component of acceleration in x direction. The column matrix, $\boldsymbol{m}_x$, is the directional mass values of the structure only.

The step by step time integration algorithm of Newmark [29] is used in conjunction with the following values for its constants: $\beta = 0.25$ and $\gamma = 0.5$. An iterative procedure is implemented to solve Equation (4) over time step $[t, t+\Delta t]$ by solving a sequence of linearized problems of the form:

$$\boldsymbol{K}^* \Delta \boldsymbol{u}^{i+1} = \boldsymbol{r}^i, \quad i = 1, 2, ... \tag{5}$$

where

$$\boldsymbol{K}^* = \boldsymbol{K}_T^i + \frac{1}{\beta (\Delta t)^2} \boldsymbol{M} + \frac{\gamma}{\beta \Delta t} \boldsymbol{C} \tag{6}$$

$$\boldsymbol{r}^i = -\boldsymbol{m}_x \ddot{\boldsymbol{u}}_{g,x}(t+\Delta t) - \boldsymbol{F}(t) - \hat{a}\, \dot{\boldsymbol{u}}_t^i - \hat{b}\, \ddot{\boldsymbol{u}}_t^i \tag{7}$$

$$\hat{a} = \frac{1}{\beta \Delta t} \boldsymbol{M} + \frac{1}{\beta} \boldsymbol{C}\ ;\ \hat{b} = \frac{1}{2\beta} \boldsymbol{M} + \Delta t \left(\frac{\gamma}{2\beta} - 1\right) \boldsymbol{C} \tag{8}$$

By solving Equation (4), the vector of the relative displacements, $\boldsymbol{u}_{t+\Delta t}^{i+1}$, in $(i+1)$th step of the iterative procedure for SSI system can be determined. Other nonlinear dynamic responses of SSI system used in definitions of limit states for each performance level are calculated using the vector of the relative displacements.

3.2 Finite element model of SSI system

Finite element model of SSI system depicted in Figure 1 is established using OpenSees, a structural analysis software framework specialized for nonlinear analyses [30]. The soil is layered with constant material properties along its depth, and the foundation is considered as rigid strip footing. Beams and columns of the structure are modelled using force-based nonlinear beam-column element that considers the spread plasticity along element's length. The integration along each element is based on Gauss-Lobatto quadrature rule.

Kent-Scott-Park model [31] is used as the confined and unconfined concrete constitutive model. The constitutive parameters of this model are: f_c=concrete peak strength in compression, f_u=residual strength, ε_0=strain at peak strength, and ε_u=ultimate compressive strain (Figure 2(a)). The concrete of cover and core in cross-section of the columns is considered as unconfined and confined, respectively. Constitutive behaviour of the reinforcing steel is based on using the one-dimensional J_2 plasticity model with linear hardening. The material parameters defining J_2

plasticity model are: E=Young's modulus, f_y=yield strength, and H=hardening modulus (Figure 2(b)).

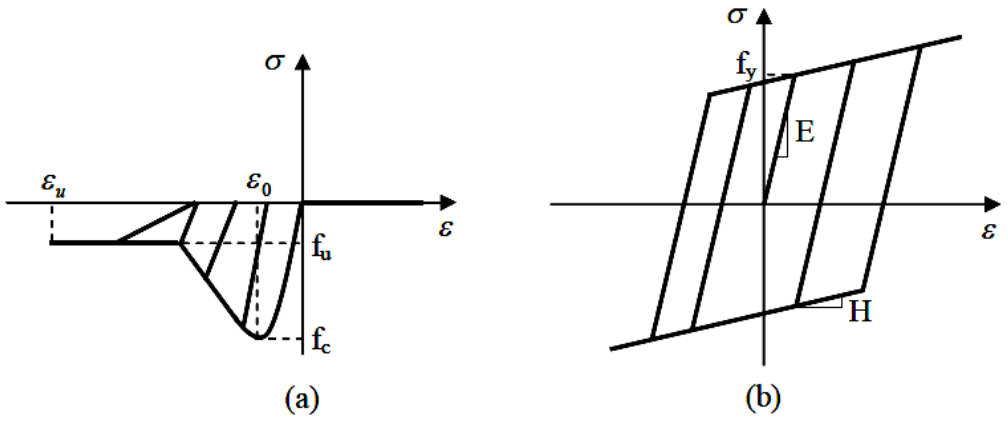

Figure 2: Material constitutive models; (a) Concrete, (b) Steel.

Soil layers are also modelled using isoperimetric four-node quadrilateral finite elements with bilinear displacement interpolation. The soil domain is assumed to be under plane strain condition with a constant soil thickness, corresponding to the inter-frame distance. The material of soil is modelled using a modified pressure-independent multi-yield-surface J_2 plasticity model [32]. This nonlinear model of soil material is described by a shear stress-strain backbone curve as shown in Figure 3. The parameters of the shear stress-strain backbone curve are expressed in [32].

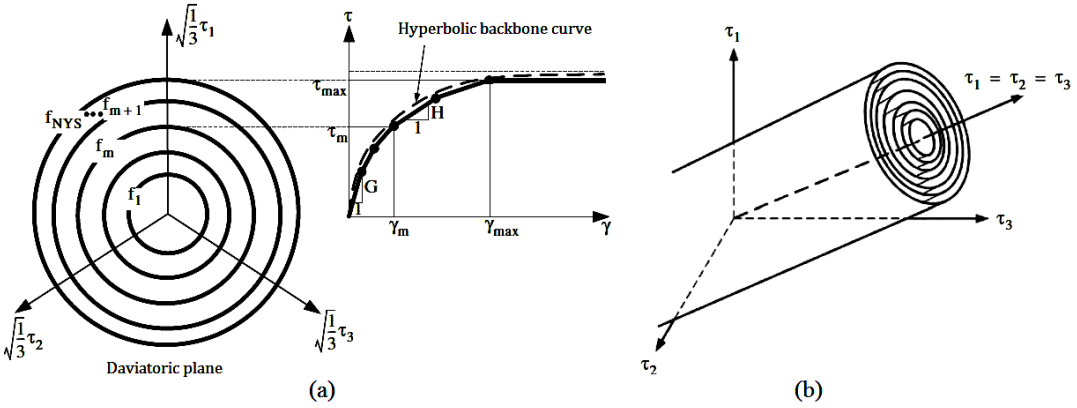

Figure 3: Yield surfaces of multi-yield-surface *J2* plasticity model; (a) Octahedral shear stress-strain, (b) Von Mises multi-yield surfaces [32].

One of the major problems in SSI system for infinite media has been modelling of the domain boundaries. Infinite boundaries have to absorb all outgoing waves and reflect no waves back into the computational domain. In this study, the standard viscous boundary proposed by Lysmer and Kuhlemeyer [34] is used for this purpose. This boundary can be described by two series of dashpots oriented normal and tangential to the boundary of a finite element mesh (Figure 1) as follows:

$$C_n = a\,\rho V_p \quad ; \quad V_p = \sqrt{\frac{2G(1-v)}{\rho(1-2v)}} \tag{9}$$

$$C_s = b\,\rho V_s \quad ; \quad V_s = \sqrt{\frac{G}{\rho}} \tag{10}$$

where C_n and C_s are the normal and shear damping, respectively; ρ and v are the mass density and Poisson ratio of soil, respectively; a and b are dimensionless parameters to be determined, and V_p and V_s are dilatational and shear wave velocity of propagation, respectively; G is low strain shear modulus. Furthermore, the soil layer is characterized by B =bulk modulus, τ =shear strength. Other parameters of soil material depend on B, G and V_p. The ZeroLength element is used for modelling the standard viscous boundary with the normal and shear damping.

The material damping matrix, $\boldsymbol{C}$, in Equation (4) of the SSI system is constructed by assembling the corresponding damping matrices of structure and soil, using the Rayleigh method [29]. The accelerated Newton algorithm based on Krylov subspaces [34] is applied for solving nonlinear equations of structural equilibrium.

4 Design optimisation of RC-MRF

In this paper, an RC-MRF is considered as a case study. Unlike the traditional design process of RC structures, a large number of design candidates can be found due to a large number of design variables. In order to find the proper design of structure, the RC frame is designed using optimisation technique, and the construction cost is considered as an objective function.

4.1 Formulation of optimisation problem

In sizing optimisation of RC frame, the aim is typically to minimize the structural weight or the construction cost of structure, under some constrains. The optimisation problem can be formulated as following:

$$\begin{aligned} &\textit{Minimize:} && F(X) \\ &\textit{Subject to:} && g_i(X) \le 0.0\,, \quad i = 1,2,\ldots,m \\ & && X_j \in R^d\,, \quad j = 1,2,\ldots,n \end{aligned} \tag{11}$$

where $F(X)$ represents objective function, $g_i(X)$ is the behavioural constraint, m and n are the number of constraints and design variables, respectively; R^d is a given set of discrete values from which the design variables X_j take values.

In this paper, the construction cost of structure has been considered as an objective function articulated as:

$$Construction\ Cost = \sum_{i=1}^{Ne} (C_C A_{Ci} L_i + C_S A_{Si} L_i + C_F A_{Fi} L_i) \quad (12)$$

where C_C and A_{Ci} are the cost per unit volume and total area of the cross-section of *i*th element related to concrete, respectively; C_S and A_{Si} are the cost per unit volume and area of steel bars in the cross-section of *i*th element; C_F and A_{Fi} are the cost per unit area of form-work and its area in the cross-section of *i*th element; L is the length of *i*th element.

4.2 Optimisation method

In this study, the DPSO algorithm proposed by Salajegheh *et al*. [10] is employed as an optimisation method. PSO has been inspired by the social behaviour of such animals as fish schooling, insects swarming and birds flocking. PSO was proposed by Kennedy and Eberhart [35] in the mid 1990s while attempting to simulate the graceful motion of bird swarms as a part of a socio-cognitive study. It involves a number of particles initialized randomly in the search space of an objective function. These particles are referred to as swarm. Each particle of the swarm represents a potential solution of the optimisation problem. The particles fly through the search space and their positions are updated based on the best positions of individual particles each iteration. The objective function is evaluated for each particle and the fitness values of particles are obtained to determine which position in the search space is the best [35]. In iteration *k*, the swarm is updated using the following equations:

$$V_i^{k+1} = w^k V_i^k + c_1 r_1 \left(P_i^k - X_i^k \right) + c_2 r_2 \left(P_g^k - X_i^k \right) \quad (13)$$

$$X_i^k = X_i^k + V_i^{k+1} \quad (14)$$

where X_i^k and V_i^k represent the current position and the velocity of the *ith* particle, respectively; P_i is the best previous position of the *ith* particle (called pbest) and P_j is the best global position among all the particles in the swarm (called *gbest*); r_1 and r_2 are two uniform random sequences generated from interval [0, 1]; w^k is the inertia weight used to discount the previous velocity of particle preserved.

Shi and Eberhart [36] proposed that the cognitive and social scaling parameters c_1 and c_2 be selected such that $c_1 = c_2 = 2.0$ to allow the product $c_1 r_1$ or $c_2 r_2$ to have a mean of 1. Each component of V_i is constrained to a maximum value defined as $V_i^{\max}$ and a minimum value defined as $V_i^{\min}$.

In the paper, the real valued model is used in DPSO. In the model, the decimal values of the design variables are used in the optimisation process instead of their binary codes. Therefore, the length of the particles is decreased and the convergence of the algorithm can be obtained with higher speed.

4.3 RC design constraints

In sizing optimisation problems of structure, the constraints are used as the design criteria. To design of structural elements, the constraints are considered based on ACI318-08 design code [37]. These constraints based on ACI318-08 are expressed as fallowing limitations:

$$M_u^{beam} \le \varphi_b M_n^{beam}; \qquad (\varphi_b = 0.9) \tag{15}$$

$$(M_u^{col}, P_u^{col}) \le (\varphi_c M_n^{col}, \varphi_c P_n^{col}); \qquad (\varphi_c = 0.65 - 0.9) \tag{16}$$

$$1\% \le \rho_{col} \le 4\% \tag{17}$$

$$\rho_{min} = max(\frac{1.4}{f_y}, \frac{0.25\sqrt{f_c}}{f_y}) \le \rho_{beam} \le \rho_{max} = (0.75(0.85\beta_1)\frac{f_c}{f_y}\frac{E_s\varepsilon_{cu}}{E_s\varepsilon_{cu} + f_y}) \tag{18}$$

$$DS = \frac{b - 2\,cover - 2\,d_{bt} - N_{bl}\,d_{bl}}{N_{bl} - 1} \ge DS_{all} \tag{19}$$

$$(b_{beam}^{top}, h_{beam}^{top}, n_{bbeam}^{top}, A_{Sbeam}^{top}) \le (b_{beam}^{bot}, h_{beam}^{bot}, n_{bbeam}^{bot}, A_{Sbeam}^{bot}) \tag{20}$$

$$(b_{col}^{top}, h_{col}^{top}, n_{bcol}^{top}, A_{Scol}^{top}) \le (b_{col}^{bot}, h_{col}^{bot}, n_{bcol}^{bot}, A_{Scol}^{bot}) \tag{21}$$

where M_u^{beam}, M_n^{beam} and φ_b are the externally applied moment, nominal flexural strength and strength reduction factor for beams, respectively; M_u^{col}, M_n^{col}, P_u^{col}, P_n^{col} and φ_c are the externally applied moment, nominal flexural strength, externally applied axial force, nominal axial strength and strength reduction factor for columns, respectively; ρ_{col}, ρ_{beam} and ρ_{min} representing the reinforcement percent (steel ratio) of cross-section of columns, the reinforcement percent of cross-section of beams and the minimum reinforcement percent of cross-section of beams, respectively; b, d_{bt}, d_{bl} and N_{bl} are width of cross-section, diameter of transverse bars, diameter and number of longitudinal bars, respectively; DS and DS_{all} are the distance among of side by side of longitudinal bars and its allowable value. The value of DS_{all} for columns and beams is defined as following:

$$DS_{all} = \begin{cases} max(25mm, d_{bl}, 1.33\,d_{\max}); & \text{for } Beams \\ max(40mm, 1.5\,d_{bl}, 1.33\,d_{\max}); & \text{for } Columns \end{cases} \tag{22}$$

where $d_{\max}$ is the diameter of greatest aggregate of concrete. Also, in Equations (19) and (20) b, h, n_b and A_s with the *top* and *bot* indices are the width, depth, number

of longitudinal bars and total area of longitudinal bars for beams and columns which are in same direction between two series storey.

Finally, based on ACI318-08 design code, the weak beam-strong column concept should be satisfied especially in seismicity zones by the following equation:

$$\frac{M_{col}^{top}+M_{col}^{bot}}{M_{beam}^{left}+M_{beam}^{right}} \geq 1.20 \tag{23}$$

where M_{col}^{top} and M_{col}^{bot} are the moment capacity of columns at the top and bottom of structural joint; also, M_{beam}^{left} and M_{beam}^{right} are the moment capacity of beams at the left and right of structural joint. Equation (23) must be satisfied for all of structural joints. Accordingly, the limitation is considered as the other constraint.

One of the most important design constraints subjected to seismic loading is the inter-storey drift ratio. The permissible ratio of the limitation is different depending upon the kind of analysis. In the paper, according to the Iranian Code of Practice for Seismic Resisting Design of Buildings (Building and Housing Research Centre) [38], permissible values related to the constraint are considered as following:

$$\begin{aligned} (\Delta_m / H) &\leq 0.025 \qquad for \;\; T < 0.7\,\text{sec} \\ (\Delta_m / H) &\leq 0.020 \qquad for \;\; T > 0.7\,\text{sec} \end{aligned} \tag{24}$$

where (Δ_m / H) representing the inter-storey drift ratio while Δ_m and H are actual values of base lateral drift and height of structure respectively; also, T is the natural period of vibration of structure.

4.4 RC design load combinations

Based on ACI318-08 code provisions, several load combination of gravity and lateral loads should be considered in line with satisfactory design. Accordingly, to simplify the design optimisation process, only five load combinations is considered as following:

$$\begin{aligned} Comb\,(1) &= 1.2\,DL + 1.6\,LL \\ Comb\,(2),(3) &= 1.2\,DL + 1.0\,LL \pm 1.4E \\ Comb\,(4),(5) &= 0.9\,DL + 1.0\,LL \pm 1.4E \end{aligned} \tag{25}$$

where DL, LL are the uniform load on beams, dead load, live load and also E is the lateral equivalent static earthquake loads acted on frame, respectively; According to [38], E can be obtained due to following lateral loading formulation:

$$F_i = \frac{w_i h_i^k}{\sum w_j h_j}(V - F_t) \tag{26}$$

in which w_i and h_i are the weight and height of *i*th story respectively; and also V and F_i are the equivalent base-shear derived from 2800-standard and equivalent static force acted on *i*th story.

5 Numerical example

5.1 Optimisation of three-bay nine-story RC-MRF

A nine-story with three-bay RC moment-resisting frames shown in Figure 4 are optimized. The group number of structural elements is presented in the Figure.

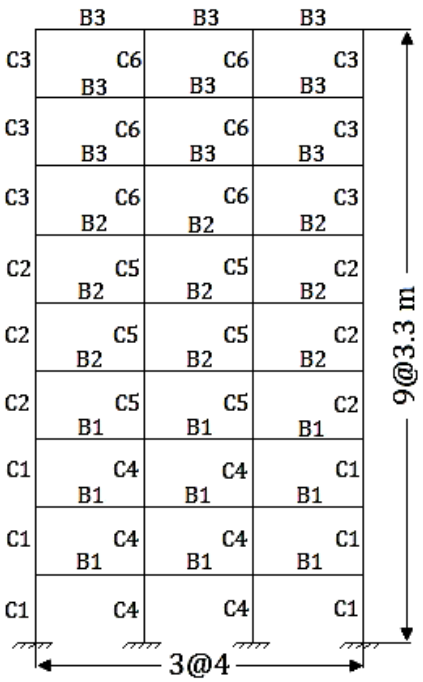

Figure 4: Nine-story three-bay RC-MRF and group number of its elements.

Two RC pre-determined cross-section databases with the necessary properties are generated for beams and columns in the optimisation procedure. The databases for beams and columns consist of several rectangular sections followed from ACI318-08 recommendations. The width of sections is chosen between 350 and 500 *mm* for beams; and between 400 and 600 *mm* for columns. Also, the height of sections is selected between 400 and 600 *mm* for beams; and between 400 and 650 *mm* for columns, respectively. The diameter of longitudinal bars is laid between 12 and 24 *mm* in the databases by step of 2 *mm*; also, in the prepared databases, the difference among the dimensions of sequentially sections 50 *mm* is considered. It is assumed that the transverse bars with 10 *mm* diameter are used for the shear control of sections. The medium ratio of section confinement is considered. In design optimisation process, effective beam and column's moment of inertia are regarded equal to 0.70 and 0.35 time of their actual values respectively.

Groups Name	Optimum Design properties		
	Width (*mm*)	Height (*mm*)	Steel Ratio (%)
C1	500	500	1.25
C2	500	500	1.25
C3	450	450	1.39
C4	500	600	1.34
C5	500	500	1.25
C6	450	500	1.24
B1	450	500	0.93
B2	450	500	0.68
B3	400	400	0.82

Table 1: Optimum properties of nine-storey three-bay frame.

5.2 Ground motion records

Six ground motion records are selected from PEER ground motion database [39] and all the records is scaled to PGA=0.6g. Some properties of the records have been listed in Table 2.

NO.	Year	Earthquake	M	USGS Class	Dist[1](*km*)	Station
1	1979	Imperial Valley	6.5	B	14.2	5051 Parachute Test Site
2	1989	LomaPrieta	6.9	B	13.0	58065 Saratoga - Aloha Ave
3	1992	Landers	7.3	B	11.6	22170 Joshua Tree
4	1994	Northridge	6.7	B	17.7	90058 Sunland - Mt Gleason Ave
5	1999	Kocaeli,	7.4	B	17.0	Arcelik
6	1999	Duzce,	7.1	B	15.6	1061ont 1061

1-Closest distance to fault rupture

Table 2: The properties of selected ground motion records.

It is noted that in the USGS classification based ground type for all records, Type B is selected and closest distance to fault rupture are selected among 11-18 *km*.

5.3 Nonlinear modelling and analysis

The analysis of RC-MRF is implemented by the finite element analysis software framework OpenSees. For modelling and analysis of structure in OpenSees, property

of materials and type of elements should be defined. In this study, *uniaxialmaterial Concrete01* shown in Figure 2(a) is used for concrete behaviour modelling. The behaviour of reinforcement bars are modelled by *uniaxialmaterial Steel01* shown in Figure 2(b). The material of soil is modelled using a modified pressure-independent multi-yield-surface J_2 plasticity model (Figure 3). The constitutive parameters of concrete, reinforcement bars and soil are shown in Table 3.

Material	Property	Value
Concrete		
	$f_c\,(MPa)$	28
	$f_u\,(MPa)$	5.97
	ε_0	0.0021
	ε_u	0.01
Steel		
	$f_y\,(MPa)$	400
	$E\,(MPa)$	210000
	H	0.01
Soil		
	$V_s\,(m/s)$	375
	$\rho\,(kN/m^3)$	17
	v	0.35

Table 3: The constitutive parameters of concrete, reinforcement bars and soil.

Beams and columns of the structure are modelled using force-based nonlinear beam-column element that considers the spread plasticity along element's length. The integration along each element is based on Gauss-Lobatto quadrature rule. The height of soil layer and the width of soil domain under structure are considered 30 *m* and 100 *m*, respectively. The soil is assumed to be under plane strain condition with a constant thickness of 3.0 *m* corresponding to the inter-frame distance. The factors of proportionality for damping matrices of structure and soil are computed by assuming 5% and 10% viscous damping for structure and soil, respectively.

5.4 Results and discussion

To evaluation of seismic behaviour of the optimized RC-MRF, as mentioned in previous sections, six ground motion records are considered. The seismic evaluation of frame is considered for each ground motion record. To achieve this purpose, non-linear time history analysis is performed using OpenSees and related results are presented. To demonstrate the effects of SSI in the non-linear response of frame, non-linear time history analysis is performed for two cases:

1) RC-MRF with SSI effects.
2) RC-MRF without SSI effects.

As mentioned, two seismic demand parameter namely inelastic inter-story drift ratio and HED distribution over the height of the frame are investigated in two cases. The profile of inelastic inter-story drift ratio and HED distribution are shown in Figures (5-10) for two cases (with SSI and without SSI).

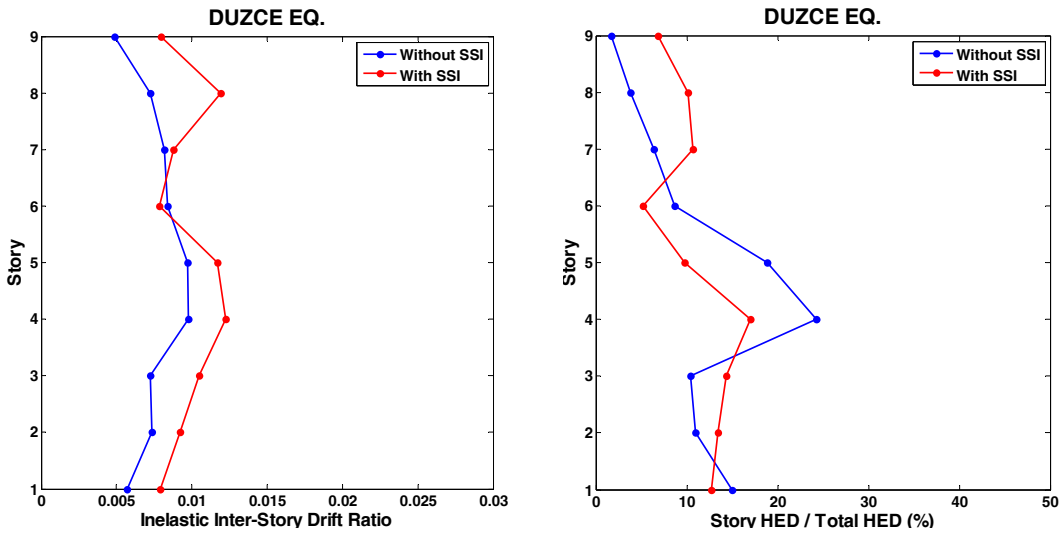

(a) (b)

Figure 5: In-elastic inter-story drift ratio (a) and Story HED/Total HED (b) – Duzce Earthquake

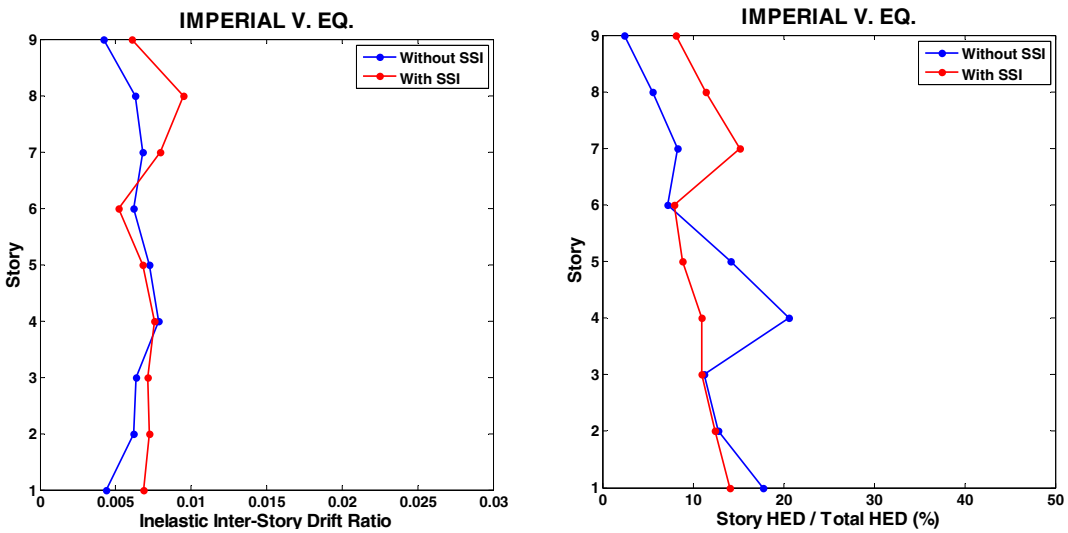

(a) (b)

Figure 6: In-elastic inter-story drift ratio (a) and Story HED/Total HED (b) – Imperial Valley Earthquake

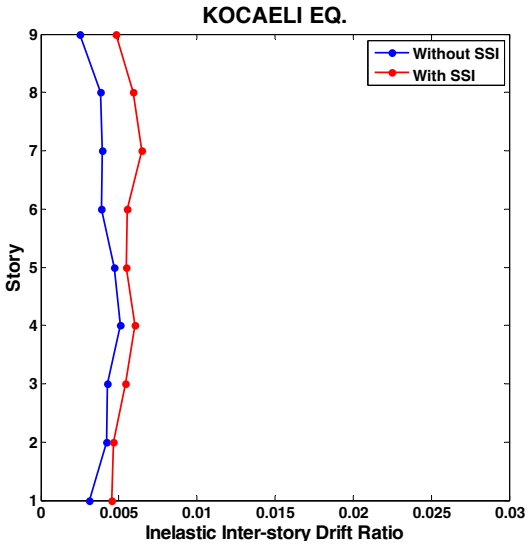

(a)

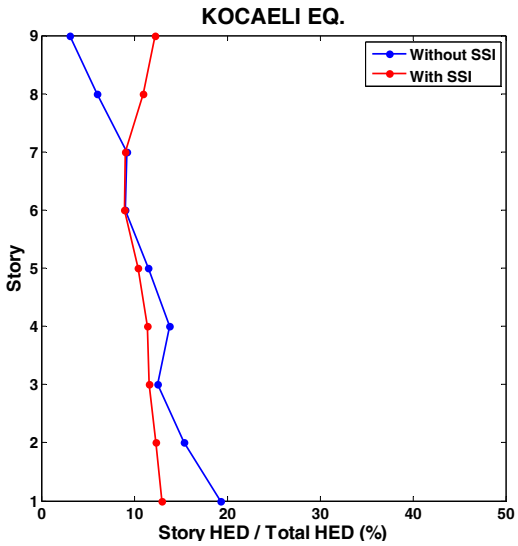

(b)

Figure 7: In-elastic inter-story drift ratio (a) and Story HED/Total HED (b) – Kocaeli Earthquake

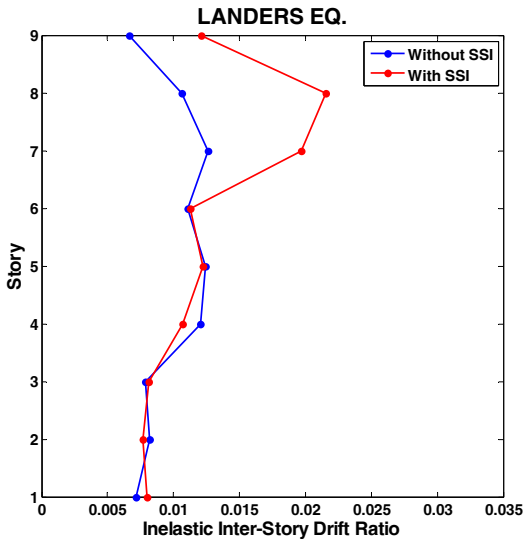

(a)

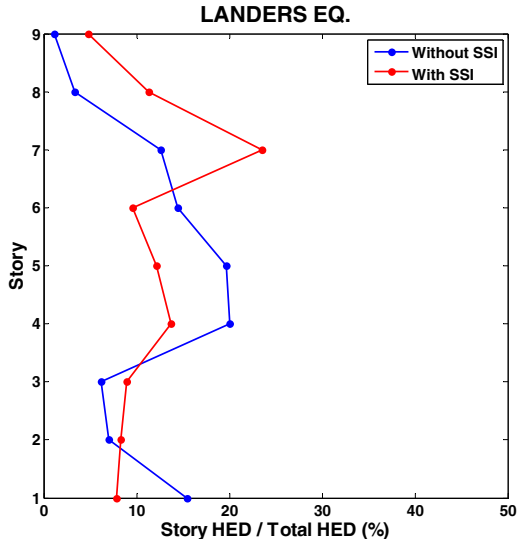

(b)

Figure 8: In-elastic inter-story drift ratio (a) and Story HED/Total HED (b) – Landers Earthquake

For example, in Imperial Valley and Landers earthquakes, the difference between case 1 and case 2 is significant. In upper stories, inelastic inter-story drift ratio has been concentrated while in without considering SSI conditions, is more uniform. In case of the investigation of HED, a ratio is defined as: the value of HED of each story to total HED that is dissipated by structure so-called Story HED/Total HED. The ratio determines the condition of HED distribution and the effects of SSI on it.

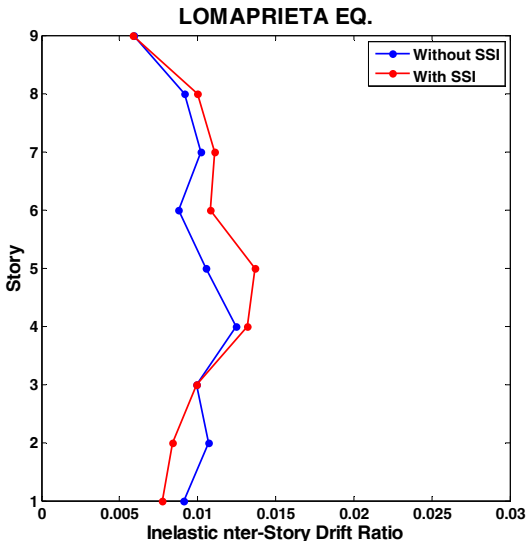

(a)

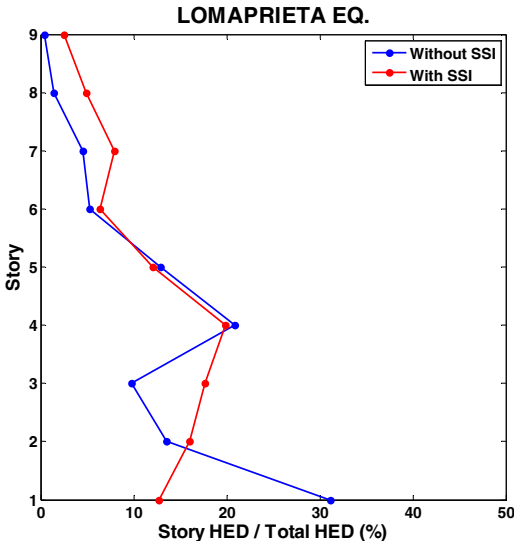

(b)

Figure 9: In-elastic inter-story drift ratio (a) and Story HED/Total HED (b) – LomaPrieta Earthquake

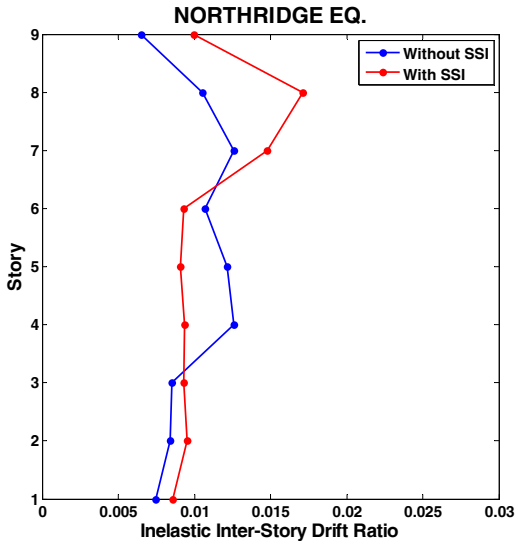

(a)

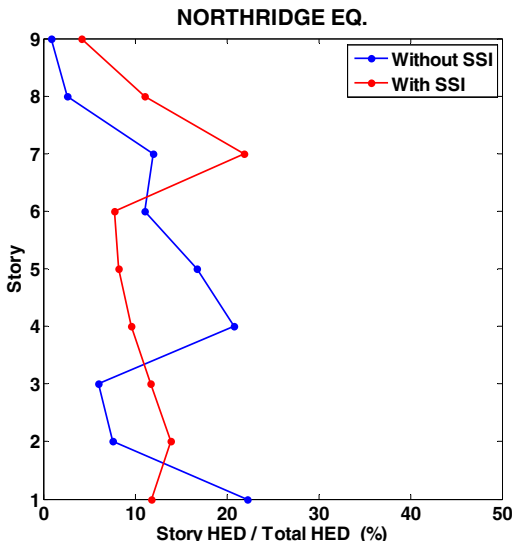

(b)

Figure 10: In-elastic inter-story drift ratio (a) and Story HED/Total HED (b) – Northridge Earthquake

As shown in Figures (5-10) for all records, there is a significant difference between the response of structure related to with considering the SSI effects and without it. A noteworthy point related to the SSI effects on HED demand, is the concentration of HED in upper stories while in the condition of without SSI the concentration has occurred in lower stories. Since HED has an approach relation with cumulative damage, the effects can be influenced on seismic performance and on the design of structure.

6 Conclusion

In this paper, a seismic evaluation of RC Moment Resistant Frames (RC-MRFs) considering soil-structure interaction (SSI) effects is presented. To achieve this purpose, a nine-story three-bay RC-MRF optimally designed based on ACI318-08 was used. To demonstrate the effects of SSI in the non-linear response of frame, non-linear time history analysis was performed for two cases, with and without SSI. In-elastic inter-storey drift ratio and hysteretic energy dissipation (HED) are utilized as non-linear responses of structure. The first response is based on displacement concepts in structures while the second response is determined based on energy concepts of structures. Currently, in addition to the force concepts, displacement concepts are of great importance in seismic evaluation and especially in PBSD of structures. In fact, HED distribution demand that leads to damage distribution in the structure during strong ground motion has been neglected. Despite the research regarding the SSI effects on structures, in this paper, both responses were considered for determining the SSI effects on the seismic behaviour of structure. The results show that, as a result of considering SSI effect, the non-linear response tolerated numerous variations. The difference between in-elastic inter-storey drift ratio pattern and HED pattern is significantly different in two cases (with and without SSI). It should be noted that HED and in fact the energy concept can be useful and efficient for seismic design of structures. Therefore, application of energy concepts should be considered in PBSD of structures.

References

[1] J.P. Wolf, S. Chongmin, "Some Cornerstones of Dynamic Soil-Structure Interaction", Engineering Structures, 24, 13-28, 2002.

[2] J.L. Wegner, M.M. Yao, X. Zhang, "Dynamic Wave-Soil-Structure Interaction Analysis in the Time Domain", Computer & Structure, 83, 2206-14, 2005.

[3] M. Nakhaei, M.A. Ghannad, "The Effect of Soil-Structure Interaction on Damage Index of Buildings", Engineering Structures, 30(6), 1491-1499, 2004.

[4] M. Eser, C. Aydemir, "The Effect of Soil-Structure Interaction on Inelastic Displacement Ratio of Structures", Structural Engineering and Mechanics, 39(5), 683-701, 2011.

[5] H.X. Lu, H.F. Jiang, P.Y. Liang, B. Wu, "Influence of Dynamic Soil-Structure Interaction on Fundamental Period for Frame Structures", Applied Mechanics and Materials, 90-93, 1618-1626, 2011.

[6] B. Fatahi, H.R. Tabatabaiefar, B. Samali, "Performance Based Assessment of Dynamic Soil-Structure Interaction Effects on Seismic Response of Building frames", in "Proceedings of the Geotechnical Risk Assessment and Management Conference", 344-351, 2011.

[7] S. Carbonari, F. Dezi, G. Leoni, "Nonlinear Seismic Behaviour of Wall-Frame Dual Systems Accounting for Soil-Structure Interaction", Earthquake Engineering & Structural Dynamics, 4, 2012 (in press).

[8] E. Sáez, F. Lopez-Caballero, A. Modaressi-Farahmand-Razavi, "Effect of The Inelastic Dynamic Soil-Structure Interaction on The Seismic Vulnerability Assessment", Structural Safety, 33(1), 51-63, 2011.

[9] E. Salajegheh, S. Gholizadeh, M. Khatibinia, "Optimal Design of Structures for Earthquake Loads by a Hybrid RBF-BPSO Method", Journal of Earthquake Engineering and Engineering Vibration, 7, 14-24, 2008.

[10] SEAOC, Vision 2000 Committee, "Performance Based Seismic Engineering of Buildings", Structural Engineers Association of California, 1995.

[11] Applied Technology Council, ATC40, "Seismic Evaluation and Retrofit of Concrete Buildings California Seismic Safety Commission", 1997.

[12] FEMA 356, "Pre standard and Commentary for the Seismic Rehabilitation of Buildings", Federal Emergency Manage Agency, prepared by the American Society of Civil Engineers, Washington, D.C., 2000.

[13] W.F. Chen, E.M. Lui, "Earthquake Engineering for Structural Design", CRC Press, 2005.

[14] Y. Bozorgnia, V.V. Bertero, "Earthquake Engineering: From Earthquake Seismology to Performance-Based Engineering", CRC Press, 2006.

[15] G.W. Housner, "Limit Design of Structures to Resist Earthquakes", in "Proceedings of the 1st World Conference on Earthquake Engineering", Earthquake Engineering Research Institute, Oakland, California, 1-13, 1956.

[16] H. Akiyama, "Earthquake Resisting Limit-State Design for Buildings", University of Tokyo Press, Tokyo, 1984.

[17] H. Kuwamura, T.V. Galambos, "Earthquake Load for Structural Reliability", Journal of Structural Engineering, ASCE, 115, 1446-1462, 1989.

[18] C.M. Uang, V.V. Bertero, "Use of Energy as a Design Criterion in Earthquake-Resistant Design", Report UBC/EERC-88/18, Earthquake Engineering Research Centre, University of California, Berkeley, CA, 1988.

[19] V.V Bertero, C.M Uang, "Issues and Future Directions in the Use of an Energy Approach for Seismic-Resistant Design of Structures", Chapter of the book, "Nonlinear Seismic Analysis and Design of Reinforced Concrete Buildings", P. Fajfar and H. Krawinkler (eds), Elsevier Applied Science 1992; 3-22.

[20] C.C. Chung, C.M. Uang, "A Procedure for Evaluating Seismic Energy Demand of Framed Structures", Earthquake Engineering and Structural Dynamics, 32, 229-244, 1990.

[21] P. Khashaee, "Energy-Based Seismic Design and Damage Assessment for Structures", Ph.D. Dissertation, Department of Civil Engineering, Southern Methodist University, USA, 2004.

[22] Workshop on Seismic Design Methodologies for the Next Generation of Codes: Conclusions and Recommendations, Last Modified, Bled, Slovenia, 1997.

[23] Y. Gong, Y. Xue, L. Xu , D.E. Grierson, "Energy-Based Design Optimisation of Steel Building Frameworks using Nonlinear Response History Analysis", Journal of Constructional Steel Research, 68, 43-50, 2012.

[24] S. Gharehbaghi, E. Salajegheh, “Optimum Distribution of Hysteretic Energy in RC Structures”, in “Proceedings of the 6th National Congress of Civil Engineering”, Semnan, Iran, 2011 (In Persian).
[25] S. Gharehbaghi, “Damage and Energy Concepts-Based Optimum Seismic Design of RC Structures”, MSc Thesis, Department of Civil Engineering, Shahid Bahonar University of Kerman, Iran, 2011 (In Persian).
[26] S. Gharehbaghi, E. Salajegheh, M. Khatibinia, “Optimisation of Reinforced Concrete Moment Resistant Frames Based on Uniform Hysteretic Energy Distribution”, in “Proceedings of the1st International Conference on Urban Construction in the Vicinity of Active Faults”, 3-5 September, Tabriz, Iran, 2011.
[27] J. Shen, B. Akbas, “Seismic Energy Demand in Steel Moment Frames”, Journal of Earthquake Engineering, 3, 519-559, 1999.
[28] K.P. Jaya, A. Meher Prasad, “Embedded Foundation in Layered Soil under Dynamic Excitations”, Soil Dynamics and Earthquake Engineering, 22, 485-98, 2002.
[29] A. Chopra, “Dynamics of Structures: Theory and Applications to Earthquake Engineering”, 3rd ed, New Jersey, Prentice Hall, 2006.
[30] OpenSees, “Open System for Earthquake Engineering Simulation”, Pacific Earthquake Engineering Research Centre (PEER), 2011.
[31] D.C. Kent, R. Park, “Flexural Members with Confined Concrete”, Journal of the Structural Division, ASCE, 97, 1969-1990, 1997.
[32] Y. Zhang, J.P. Conte, Z. Yang, A. Elgamal, J. Bielak, G. Acero, “Two-Dimensional Nonlinear Earthquake Response Analysis of a Bridge-Foundation-ground system”, Earthquake Spectra, 24(2), 343-86, 2008.
[33] J. Lysmer, R.L. Kuhlemeyer, “Finite Element Model for Infinite Media” Journal of Engineering Mechanics, ASCE, 95, 859-877, 1969.
[34] S.M. Scott, G.L. Fenves, “Krylov Subspace Accelerated Newton algorithm: Application to Dynamic Progressive Collapse Simulation of Frames”, Journal Structural Engineering, ASCE , 136, 473-80, 2010.
[35] J. Kennedy, R.C. Eberhart, “Swarm Intelligence”, Morgan Kaufman Publishers, San Francisco, 2002.
[36] Y. Shi, R.C. Eberhart, “A Modified Particle Swarm Optimizer”, in “Proceedings IEEE International Conference on Evolutionary Computation”, IEEE Press, 69-73, 1998.
[37] ACI, “Building Code Requirements for Structural Concrete (ACI 318-08) and Commentary”, American Concrete Institute, Farmington Hills, Michigan, 2008.
[38] Standard No. 2800, “Iranian Code of Practice for Seismic Resistant Design of Buildings”, 3rd ed, Building and Housing Research Centre, 2004.
[39] PEER, “PEER Column Database”, Pacific Earthquake Engineering Research Center, University of California, Berkeley, California, 2010. http://nisee.berkeley.edu/.